Control Engineering Practice 85 (2019) 132–137

Contents lists available at ScienceDirect

Control Engineering Practice

journal homepage: www.elsevier.com/locate/conengprac

State-of-charge estimation for lead–acid batteries via embeddings and observers

D. Carnevale [a], C. Possieri [b,*], M. Sassano [a]

[a] Dipartimento di Ingegneria Civile e Ingegneria Informatica, Università di Roma Tor Vergata, Via del Politecnico 1, 00133 Roma, Italy
[b] Dipartimento di Elettronica e Telecomunicazioni, Politecnico di Torino, Corso Duca degli Abruzzi 24, 10129 Torino, Italy

ARTICLE INFO

Keywords:
State-of-charge
Observer design
Nonlinear systems
Algebraic geometry
System embeddings
High-gain observers

ABSTRACT

In this paper, an approach is proposed to estimate the open-circuit voltage of a battery – and consequently the battery State-of-Charge during normal operation of electric vehicles – by only measuring the charge/discharge current and the voltage on the load. The result is achieved, without any knowledge of the characteristic values of the battery model, by combining a *system embedding* with a *high-gain observer design* strategy. Interestingly, the method is based on genuinely nonlinear estimation strategies, hence it does not suffer the typical drawbacks of linear approaches, including the requirement for *persistence of excitation* of the charge/discharge current.

1. Introduction

One of the most critical challenges for energy sustainability in the near future consists in replacing internal combustion engine vehicles with electric, possibly autonomous, vehicles (Bartlett et al., 2016; Corno, Bhatt, Savaresi, & Verhaegen, 2015; Partovibakhsh & Liu, 2015; Piller, Perrin, & Jossen, 2001). Towards this objective, several issues must still be tackled, including efficient managing and monitoring of the batteries required for energy storage in electric vehicles. In fact, differently from internal combustion engine cars, the estimation of the battery state of charge (SOC) is a challenging problem, both from the practical as well as the conceptual point of view (Chiasson & Vairamohan, 2003; Pang, Farrell, Du, & Barth, 2001). The task is rendered daunting by the peculiar usage of the batteries in heavy duty vehicles (*e.g.*, forklifts) that are characterized by repeated charge/discharge cycles before a complete discharge of the battery, which would permit a reset of the SOC estimate to a known value (Pang et al., 2001).

Since maintaining the state of charge within desired bounds is crucial for safety and efficiency reasons, several approaches to estimate the SOC of the battery have been defined, see *e.g.* Pang et al. (2001), Chiasson and Vairamohan (2003). The SOC can be defined, for instance, by considering a completely discharged battery and by letting $I_b(t)$ denote the charging current. Then, the SOC is clearly given by

$$\mathrm{SOC}(t) \triangleq \frac{1}{Q_0}\int_{t_0}^{t} I_b(\tau)d\tau\,, \tag{1}$$

where Q_0 denotes the total charge that the battery can hold. However, the method discussed above is seriously hindered by the presence of pure integration, which is particularly subject to biases, numerical errors, and the non-perfect knowledge of the (very slowly time-varying) parameter Q_0. To circumvent this issue, it has been shown in Pang et al. (2001), Chiasson and Vairamohan (2005) and Coleman, Lee, Zhu, and Hurley (2007) that, when dealing with lead–acid batteries, there is an approximately linear relation between the SOC and its open-circuit voltage V_{oc},

$$V_{oc}(t) = a_1\mathrm{SOC}(t) + a_0,$$

which immediately leads to the estimate

$$\mathrm{SOC}(t) = a_1^{-1}(V_{oc}(t) - a_0)\,, \tag{2}$$

where a_0 is the battery terminal voltage (that can be determined by measuring V_{oc} when SOC $= 0$, *i.e.*, when the battery is completely discharged) and a_1 is related to the value of a_0 and V_{oc} (namely, it is the difference between V_{oc} and a_0 when SOC $= 1$, *i.e.*, when the battery is fully charged). The focus is therefore shifted towards the estimation of V_{oc}, which clearly cannot be directly measured during normal operation of an electric vehicle, since, to do so, the battery must be disconnected from the load. Note that, since the attention is focused on V_{oc}, the given techniques can be used even if the dependence of SOC on V_{oc} is nonlinear (Fuller, Doyle, & Newman, 1994; Plett, 2004; Smith & Wang, 2006).

The main contribution of this paper consists in a systematic approach that allows to estimate the open-circuit voltage $V_{oc}(t)$ of a battery during operation. Such a result is achieved by measuring the charge/discharge voltage and current on the load, without assuming any knowledge on the nominal values of the battery parameters. Namely, by using a well established nonlinear dynamical model of a battery taken from

* Corresponding author.
E-mail addresses: daniele.carnevale@uniroma2.it (D. Carnevale), corrado.possieri@uniroma2.it (C. Possieri), mario.sassano@uniroma2.it (M. Sassano).

https://doi.org/10.1016/j.conengprac.2019.01.011
Received 20 February 2018; Received in revised form 10 December 2018; Accepted 15 January 2019
Available online 6 February 2019

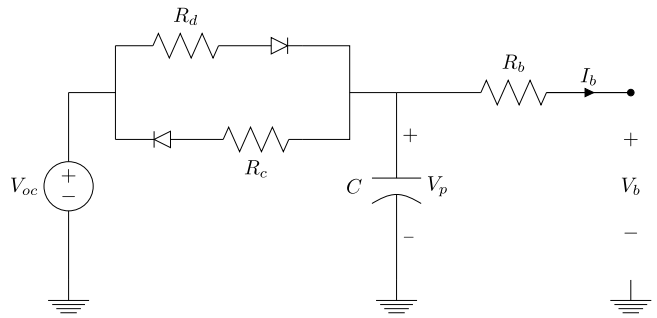

Fig. 1. Battery model with internal charge/discharge resistance and electrolytic diffusion.

the literature (Chiasson & Vairamohan, 2003; Pang et al., 2001), the techniques proposed in Menini, Possieri, and Tornambe (2016) (embeddings of the nonlinear system) are employed to obtain formulas that relate the measured quantities (*i.e.*, the load current and voltage) and their time derivatives with the open circuit voltage V_{oc}. The main innovation of the given method with respect to the existing ones – as Kalman filtering (Barbarisi, Vasca, & Glielmo, 2006; Paschero, Storti, Rizzi, Mascioli, & Rizzoni, 2016; Santhanagopalan & White, 2006) and other linearized techniques (see Chang (2013) and references therein for a detailed review of techniques for state of charge estimation) – is that it is genuinely nonlinear and hence it does not require the assumptions of classical linear identification approaches applied to intrinsically nonlinear problems as, *e.g.*, *persistence of excitation* of the load current and voltage. In particular, the combination of innovative techniques borrowed from algebraic geometry and the use of filtered high-gain observers, together with the description of an extremely low-cost setup to test observers for State-Of-Charge estimation, may bring a different and novel point of view on such a challenging problem. Several experiments that validate and corroborate the proposed technique are reported.

The remainder of the paper is organized as follows. The model of the battery employed herein is introduced and discussed in Section 2, while the observer design strategy is comprehensively described in Section 3. Finally, the experimental set-up and several practical case studies are the topics of Sections 4, 5.1 and 5.2, respectively.

2. Dynamical model of a battery

The battery model considered in this paper is described by the circuit depicted in Fig. 1 (Bhangu, Bentley, Stone, & Bingham, 2005; Chiasson & Vairamohan, 2003; Pang et al., 2001). More precisely, V_{oc} denotes the open-circuit voltage, whereas R_c and R_d are employed to distinguish the internal constant resistance of the battery during the charge or discharge phases, respectively. Clearly, the presence of the diodes in the circuit ensures that only one of the two resistances has current flowing at any given time instant. In addition, a capacitor is added to model the diffusion of electrolytic through the battery and the corresponding effect of inducing currents within the battery (Chiasson & Vairamohan, 2003). Finally, V_b denotes the battery terminal voltage. It is assumed that all the parameters involved in the definition of the battery model are constant but *unknown* values.

By defining the (extended) state variables (Chiasson & Vairamohan, 2003)

$$x_1 = V_p, \qquad x_2 = \frac{1}{R_x C}, \qquad x_3 = \frac{V_{oc}}{R_x C}, \qquad x_4 = \frac{1}{C}, \qquad x_5 = R_b,$$

where R_x stands for R_c during charge and R_d during discharge. The model of the lead–acid battery can be derived as follows

$$\dot{x}_1 = -x_1 x_2 + x_3 - I_b(t) x_4, \tag{3a}$$
$$\dot{x}_2 = 0, \tag{3b}$$
$$\dot{x}_3 = 0, \tag{3c}$$
$$\dot{x}_4 = 0, \tag{3d}$$
$$\dot{x}_5 = 0, \tag{3e}$$
$$V_b = x_1 - I_b(t) x_5. \tag{3f}$$

The initial condition $\mathbf{x}(0)$ of system (3) is unknown. The objective of this paper is to estimate the voltage $V_{oc} = \frac{x_3}{x_2}$ of the circuit depicted in Fig. 3 (which can be related to SOC through (2)) by only measuring $V_b(t)$ and $I_b(t)$.

Remark 1. The states x_2, x_3, x_4, x_5 of system (3) can be considered as slow-varying inputs to be estimated. In fact, the system parameters (including V_{oc}) may slowly vary due to operating conditions and aging processes. However, the method given in Section 3 is robust with respect to these variations, since it does not require any knowledge of such states. ▲

The structure of the system (3) and of the control objective is deceptively simple: the battery model (3) is a nonlinear time-varying system, hence also the definition of *observability* must be carefully considered. In particular, while essentially linear tools, involving the Observability Gramian, are employed in Pang et al. (2001) and Chiasson and Vairamohan (2003), herein the approach is based on genuinely nonlinear techniques, which do not suffer the typical drawbacks of intrinsically linear strategies, such as *persistence of excitation*. More precisely, the notion of observability for (3) considered in this paper is introduced in the following definition.

Definition 1. (Observability Rank Condition (Isidori, 1995)). Consider a nonlinear system described by the equations $\dot{\mathbf{x}} = f(\mathbf{x}, \mathbf{u})$, $y = h(\mathbf{x}, \mathbf{u})$, with $\mathbf{x}(t) \in \mathbb{R}^n$, $\mathbf{u}(t) \in \mathbb{R}^m$ and $\mathbf{y}(t) \in \mathbb{R}^p$, and define the observability mapping $\mathcal{O}_k : \mathbb{R}^n \times \mathbb{R}^m \to \mathbb{R}^k$ as

$$\mathcal{O}_k(\mathbf{x}, \mathbf{u}) = \begin{bmatrix} \mathbf{y} & \dot{\mathbf{y}} & \cdots & \mathbf{y}^{(k-1)} \end{bmatrix}^\top. \tag{4}$$

The system is locally uniformly observable around $\mathbf{x}_0 \in \mathbb{R}^n$ if there exists $k \geqslant n$ such that the differential $d\mathcal{O}_k(\mathbf{x}_0, \mathbf{u})$ is non-singular, namely such that $\mathcal{O}_k(\mathbf{x}, \mathbf{u})$ is locally injective. ∘

Once the observability rank condition above is satisfied, hence injective and invertibility of the mapping $\mathcal{O}_k$ is insured, the observer design task can be accomplished by first estimating the time derivatives of the output $\mathbf{y}$ (and possibly of the controlled/exogenous inputs) and then inverting the equations in (4) to determine expressions for the components of the state $\mathbf{x}$. While the first task is carried out by means of rather standard high-gain techniques, the latter is typically the stumbling block of the overall estimation strategy. Herein, this issue is circumvented, for the first time in the literature, by relying on algebraic geometric tools that allow to express the inverse mapping in *closed-form*, as comprehensively discussed in the following section.

3. Battery state of charge estimation

In this section, an observer design strategy for the battery model depicted in Fig. 1 is proposed. Such an observer is based on the techniques illustrated in Menini et al. (2016) and hence, for the notation and theoretical results behind the procedure outlined in this section the interested reader is referred to Menini et al. (2016).

Let $y = V_b$ and $u = I_b$ denote the output and the input of the model, respectively. Then, the system (3) is a nonlinear, as a matter of fact polynomial, single-input, single-output plant and hence the techniques proposed in Menini et al. (2016), Menini, Possieri, and Tornambe (2015a) and Menini, Possieri, and Tornambe (2015b) can be used to design an observer for system (3). Towards this end, consider

the observability map of order 5 for system (3), namely, letting $\mathbf{u}_{e,4} = [\ u_0 \quad \dots \quad u_4\ ]^\top$,

$$\mathcal{O}_4(\mathbf{x}, \mathbf{u}_{e,4}) = \begin{bmatrix} x_1 - u_0 x_5 \\ -u_0 x_4 - u_1 x_5 - x_1 x_2 + x_3 \\ x_2(u_0 x_4 - x_3) - u_1 x_4 - u_2 x_5 + x_1 x_2^2 \\ x_2^2(-u_0 x_4 - x_1 x_2 + x_3) + u_1 x_4 x_2 - u_2 x_4 - u_3 x_5 \\ x_2^3(u_0 x_4 + x_1 x_2 - x_3) - u_1 x_4 x_2^2 + u_2 x_4 x_2 - u_3 x_4 - u_4 x_5 \end{bmatrix},$$

where $u_i = \frac{d^i}{dt^i} u(t)$, $i = 0, \dots, 4$ denote the time derivative of the input $u(t)$. As anticipated in the definition of the Observability Rank Condition, the mapping $\mathcal{O}_4$ essentially relates the components of the state $\mathbf{x} = [\ x_1 \quad \dots \quad x_5\ ]^\top$ of system (3) and the time derivatives of the input u with the output y and its time derivatives. In fact, letting $\mathbf{x}(t)$ be the solution to system (3) $\mathbf{u}_{e,4}(t) = [\ u(t) \quad \cdots \quad \frac{d^4}{dt^4} u(t)\ ]^\top$, and $\mathbf{y}_{e,4}(t) = [\ y(t) \quad \cdots \quad \frac{d^4}{dt^4} y(t)\ ]^\top$, one has that

$$\mathbf{y}_{e,4}(t) = \mathcal{O}_4(\mathbf{x}(t), \mathbf{u}_{e,4}(t)), \quad \text{for all admissible } t \geqslant 0.$$

In order to satisfy the requirements of Definition 1, it can be easily verified that the mapping $\mathbf{x} \mapsto \mathcal{O}_4(\mathbf{x}, \mathbf{u}_{e,4})$ is locally invertible in a neighborhood of almost any point in $\mathbb{R}^5$ for a "generic" $\mathbf{u}_{e,4}$: in other words, $d\mathcal{O}_4(\mathbf{x}, \mathbf{u}_{e,4})$ has full rank for almost all the $(\mathbf{x}, \mathbf{u}_{e,4}) \in \mathbb{R}^5 \times \mathbb{R}^5$. Hence, the technique illustrated in Menini et al. (2016) and Possieri and Busetto (2017) can be employed to determine a closed-form expression for the inverse of the mapping $\mathbf{x} \mapsto \mathcal{O}_4(\mathbf{x}, \mathbf{u}_{e,4})$. In such a way, the state of system (3) can be reconstructed from measurements of the time derivatives of I_b and V_b. Thus, letting $\mathbf{y}_{e,4} := [\ y_0 \quad \dots \quad y_4\ ]^\top$ define the ideal (for the formal definition of an ideal, see Cox, Little, and O'Shea (2015)

$$\mathcal{J} = \langle \mathbf{y}_{e,4} - \mathcal{O}_4(\mathbf{x}, \mathbf{u}_{e,4}) \in \mathbb{R}[\mathbf{x}, \mathbf{u}_{e,4}, \mathbf{y}_{e,4}] \rangle.$$

Hence, let $\mathcal{G}_i$ be a Groebner basis of $\mathcal{J}$ according to a monomial order that eliminates all the $\mathbf{x}$'s apart from x_i and consider $\mathcal{G}_i \cap \mathbb{R}[x_i, \mathbf{u}_{e,4}, \mathbf{y}_{e,4}]$, $i = 1, \dots, 4$. It follows that for each $i \in \{1, \dots, 4\}$ there exists a polynomial g_i such that $\{g_i\} = \mathcal{G}_i \cap \mathbb{R}[x_i, \mathbf{u}_{e,4}, \mathbf{y}_{e,4}]$ and $\mathrm{LM}(g_i) = \eta x_i$, where $\eta \in \mathbb{R}[x_i, \mathbf{u}_{e,4}, \mathbf{y}_{e,4}]$. Namely, the polynomial g_i is an x_i-dependent *embedding* of system (3), *i.e.*, g_i vanish identically if computed along the trajectories of system (3),

$$g_i(x_i(t), \mathbf{y}_{e,4}(t)) = 0, \quad \forall t \geqslant 0, \quad i = 1, \dots, 5.$$

Then, by Proposition 2 of Menini et al. (2016), such polynomials can be used to obtain a rational mapping $(\mathbf{u}_{e,4}, \mathbf{y}_{e,4}) \mapsto \mathbf{x}$ that allows to reconstruct the state $\mathbf{x}$ of system (3) from the knowledge of the time derivatives of I_b and V_b. Namely, by inspecting the polynomials g_i, such a mapping is given by

$$x_1 = \frac{\varrho_1(\mathbf{u}_{e,4}, \mathbf{y}_{e,4})}{u_2^2 y_3 - u_4 u_2 y_1 + u_3^2 y_1 + u_1 u_4 y_2 - u_3(u_2 y_2 + u_1 y_3)}, \tag{5a}$$

$$x_2 = \frac{-u_2^2 y_4 - u_3^2 y_2 + u_4(u_2 y_2 - u_1 y_3) + u_3(u_2 y_3 + u_1 y_4)}{u_2^2 y_3 - u_4 u_2 y_1 + u_3^2 y_1 + u_1 u_4 y_2 - u_3(u_2 y_2 + u_1 y_3)}, \tag{5b}$$

$$x_3 = \frac{\varrho_2(\mathbf{u}_{e,4}, \mathbf{y}_{e,4})}{u_2^2 y_3 - u_4 u_2 y_1 + u_3^2 y_1 + u_1 u_4 y_2 - u_3(u_2 y_2 + u_1 y_3)}, \tag{5c}$$

$$x_4 = \frac{\varrho_3(\mathbf{u}_{e,4}, \mathbf{y}_{e,4})}{(u_2^2 y_3 - u_4 u_2 y_1 + u_3^2 y_1 + u_1 u_4 y_2 - u_3(u_2 y_2 + u_1 y_3))^2}, \tag{5d}$$

$$x_5 = \frac{u_3(y_2^2 - y_1 y_3) + u_2(y_1 y_4 - y_2 y_3) + u_1(y_3^2 - y_2 y_4)}{u_2^2 y_3 - u_4 u_2 y_1 + u_3^2 y_1 + u_1 u_4 y_2 - u_3(u_2 y_2 + u_1 y_3)}, \tag{5e}$$

where $\varrho_1, \varrho_2, \varrho_3$ are polynomials in $\mathbb{R}[\mathbf{u}_{e,4}, \mathbf{y}_{e,4}]$.

Remark 2. The inverse of the observability map $\mathcal{O}_4$ in (5) is well-defined whenever the common denominator does not vanish. Note that such polynomial, with y_i substituted by the ith entry of the observability map $\mathcal{O}_4(\mathbf{x}, \mathbf{u}_{e,4})$, $i = 0, \dots, 4$, equals $\det(d\mathcal{O}_k(\mathbf{x}_0, \mathbf{u}_{e,4}))$, and hence the formulas given in (5) can be used whenever system (3) is locally observable. Moreover, the set of all the $(\mathbf{u}_{e,4}, \mathbf{y}_{e,4})$ such that the denominator vanishes has zero measure in $\mathbb{R}^5 \times \mathbb{R}^5$. Therefore, the formulas in (5) constitute an almost global inverse of $\mathcal{O}_4$. ▲

The expressions given in (5) relate the current time derivatives of I_b and V_b with the state of system (3) and can be used to analyze the sensitivity of the given technique with respect to errors in the estimates of $\mathbf{u}_{e,4}$ and $\mathbf{y}_{e,4}$. It is worth mentioning that, for a generic choice of the input $u(t)$, the denominator of such rational quantities is not identically zero. In fact, as stated in Sussmann (1978), for polynomial systems, in the class on smooth inputs, universality (*i.e.*, the capability of reconstructing the state of a system from the knowledge of the output and input) is a generic property and, for the considered system, an input is universal if it is such that the polynomial function $u_2^2 y_3 - u_4 u_2 y_1 + u_3^2 y_1 + u_1 u_4 y_2 - u_3(u_2 y_2 + u_1 y_3)$ does not vanish over non-empty time intervals. This property can be easily tested since solutions to system (3) can be actually determined by simple integration. Hence, an expression $\Phi(\mathbf{u}_{e,4}, \mathbf{y}_{e,4})$ of V_{oc} as a function of $\mathbf{u}_{e,4}$ and $\mathbf{y}_{e,4}$ can be obtained, by using the inverse of $\mathcal{O}_4(\mathbf{x}, \mathbf{u}_{e,4})$, that is

$$\Phi := \frac{\varrho_2(\mathbf{u}_{e,4}, \mathbf{y}_{e,4})}{-u_2^2 y_4 - u_3^2 y_2 + u_4(u_2 y_2 - u_1 y_3) + u_3(u_2 y_3 + u_1 y_4)}. \tag{6}$$

Note now that $\mathbf{u}_{e,4}$ and $\mathbf{y}_{e,4}$ are typically not directly measurable and hence there is the need for a tool capable of estimating them. In this work, high gain "practical" observers are used to achieve this objective. Namely, let $\xi(t)$ be a signal and consider its fourth-order time derivative $\frac{d^4}{dt^4}\xi(t)$. If there exists $M \in \mathbb{R}$ such that $|\frac{d^4}{dt^4}\xi(t)| < M$ for all $t \geq 0$, then, by Tornambe (1992, Thm. 2) a high-gain "practical" observer for the time derivatives of the signal $\xi(t)$ up to the 4th order is given by

$$\dot{\hat{\xi}}_0 = \hat{\xi}_1 + \frac{\kappa_1}{\varepsilon}(\xi - \hat{\xi}_0), \tag{7a}$$

$$\vdots$$

$$\dot{\hat{\xi}}_3 = \hat{\xi}_4 + \frac{\kappa_4}{\varepsilon^4}(\xi - \hat{\xi}_0), \tag{7b}$$

$$\dot{\hat{\xi}}_4 = \frac{\kappa_5}{\varepsilon^5}(\xi - \hat{\xi}_0), \tag{7c}$$

where $\kappa_1, \dots, \kappa_5$ are such that $\lambda^5 + \kappa_1 \lambda^4 + \cdots + \kappa_5$ is Hurwitz, $\varepsilon > 0$ is a sufficiently small parameter, and $\hat{\xi}_i$ is an estimate of $\frac{d^i}{dt^i}\xi(t)$, $i = 0, \dots, 4$. Since the constant M can be arbitrarily large, the assumption about $\frac{d^4}{dt^4}\xi(t)$ holds for many classes of real-world signals (*e.g.*, sinusoids, pseudo-pulses, *etc.*).

Hence, two systems of the form given in (7) can be used to estimate $\mathbf{u}_{e,4}$ and $\mathbf{y}_{e,4}$, provided the above boundedness assumption on the higher-order derivatives holds.

Therefore, by combining the high-gain observer (7), the closed-form expression of the inverse of the observability mapping given in (5), and the expression of V_{oc} given in (6), an observer for the state of charge of the battery can be obtained. However, since the signals y and u may be affected by additive noise and u may be such that the denominator of the expressions given in (5) vanishes for isolated time instants, in the following practical experiments the signals y and u have been filtered with low pass filters. The filtered output is then fed to the high-gain observers to estimate their time derivatives. The latter are then used to estimate V_{oc} by mean of (6) and another low pass filter to deal with possible isolated singularities of the expression given in (6). Therefore, the proposed observer for V_{oc} has the form depicted in Fig. 2. Note that such an observer design strategy does not require the knowledge of any parameter of the circuit in Fig. 1.

The output $\hat{V}_{oc}$ of the observation scheme reported in Fig. 2 is an estimate of V_{oc} and hence, by Pang et al. (2001), an estimate of the SOC is given by the expression given in (2) (or any other given relation between SOC and V_{oc}).

In the following section the experimental setup, which has been employed to validate the performance of the proposed observer design technique, is described.

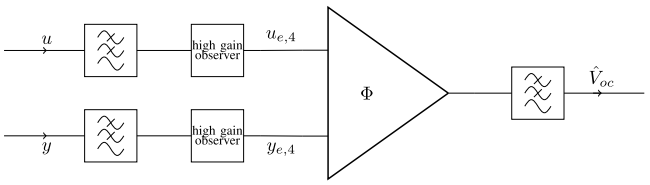

Fig. 2. Proposed observer scheme for V_{oc}, consisting of high-gain observers to estimate the time derivatives of the input, $u(t) = I_b(t)$, and the output, $y(t) = V_b(t)$, of the battery, and the closed-form expression Φ of the inverse of the observability mapping obtained by means of algebraic geometry tools.

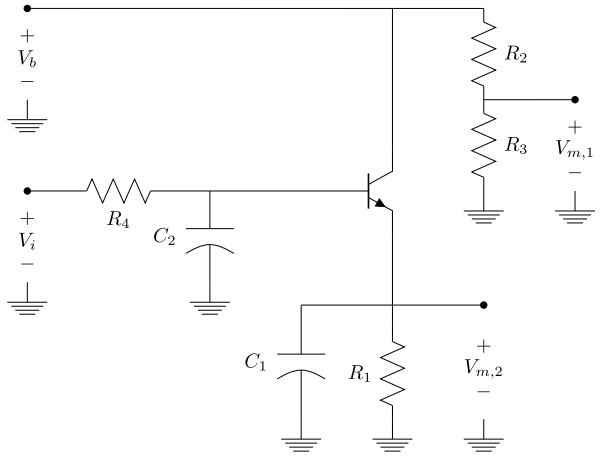

Fig. 3. Scheme of the circuit employed to measure I_b and V_b, where a transistor is driven in order to provide a variable load to the battery.

4. Experimental setup

In order to corroborate the theoretical claims of the observer design scheme proposed in Section 3, practical experiments have been carried out both with an actual battery and with an "emulated" one (see Section 5).

In Chiasson and Vairamohan (2003), it has been proved that V_{oc} is not observable from measurements of $y(t)$ and $u(t)$ if $\frac{d^2}{dt^2}u(t) \neq 0$ in a non-empty time interval. Interestingly, such a result is confirmed also by the expressions given in (5) for the inverse of the observability map that are not defined if $u_2 = 0$, $u_3 = 0$, and $u_4 = 0$. Therefore, in order to absorb a non-constant current from the battery and to measure I_b and V_b, the circuit depicted in Fig. 3 has been realized in order to provide a variable (controlled) resistive load to the battery.

By applying a non-constant voltage to the port V_i and plugging the battery to the port V_b, a non-constant current I_b is absorbed by the battery. In order to measure both V_b and I_b, the voltages $V_{m,1}$ and $V_{m,2}$ have been measured. Note that, given the limitations of the data acquisition hardware, a current divider has been used to obtain $V_{m,1}$, so that

$$V_b = \frac{R_2 + R_3}{R_3} V_{m,1}, \qquad I_b = \frac{V_{m,2}}{R_1} + \frac{\dot{V}_{m,2}}{C_1}. \tag{8}$$

In the following, in order to simplify the mathematical machinery behind the proposed estimation technique, I_b has been approximated as $I_b \simeq V_{m,2}/R_1$ due to the facts that $1/C_1$ is large because of the small capacitance used and that $\dot{V}_{m,2}$ is small since the circuit is operated at low frequency (namely, 0.2778 Hz).

The values of the component that have been used to realize the circuit depicted in Fig. 3 are reported in Table 1 for completeness, but the knowledge of their values has not been used to carry our the experiments reported in Section 5.

In the experiments reported in the subsequent Section 5, an Arduino Uno has been used to generate V_i (using PWM signals and a standard low-pass filter with capacitor 100 μF and resistance 10 KΩ) and to collect the measurements $V_{m,1}$ and $V_{m,2}$. The Arduino communicated through the serial port with a laptop running Windows 8.1, with an Intel Core i5 3210M CPU (2.50 GHz) processor and 6 GB of RAM DDR3. The observer proposed in Section 3 has been implemented in Matlab 2013a by integrating the corresponding differential equation through the direct Euler method.[1] Interestingly, the overall estimation algorithm can be effectively run in real-time with respect to the collection of the measured values of the load current and voltage.

Table 1
Components used to realize the circuit in Fig. 3.

R_1	10 Ω ± 1%	C_1	22 μF
R_2	20 KΩ ± 1%	C_2	100 μF
R_3	10 KΩ ± 1%	BJT	BD139
R_4	10 KΩ ± 1%	Micro	Arduino Uno

Table 2
Components used to realize the circuit in Fig. 1.

Voltage source	GW Instek GPC-3030DQ
R_d	0.6 Ω ± 1%
C	220 μF
R_b	0.3 Ω ± 1%

5. Experimental results

In this section, the results of some numerical experiments performed to test the proposed observer are reported. In order to validate the given technique to estimate the state of charge of a battery, the proposed observer is first tested through an "emulated" battery for which the parameter V_{oc} is actually measurable. Secondly, the proposed technique is applied to estimate the state of charge of an actual battery.

5.1. "Emulated" battery

In order to test the proposed estimation technique the circuit depicted in Fig. 1 has been realized with the components reported in the following Table 2, so that the circuit parameter V_{oc} can be directly measured while it is estimated through the technique proposed in Section 3. This allowed us to test the effectiveness of the proposed estimation method in an experimental setting. In the reported examples, the actual voltage V_{oc} has been measured with the same Arduino Uno used to generate V_i and to measure $V_{m,1}$, $V_{m,2}$.

Several experiments have been carried out by modifying the duty cycle of the PWM available on the Arduino board with amplitude 5 V and frequency 0.2778 Hz. The voltages $V_{m,1}$ and $V_{m,2}$ have been acquired with a sample frequency of 100 Hz and the expressions in (8) have been used to determine $u = I_b$ and $y = V_b$. Hence, the ODEs corresponding to the observer depicted in Figure (7) have been integrated by using the Euler direct method with a sampling time equal to 0.01 s. The parameters of both the high-gain observer have been set to $\varepsilon = 0.4$, $\kappa_1 = 5$, $\kappa_2 = 10$, $\kappa_3 = 10$, $\kappa_4 = 5$, $\kappa_5 = 1$, so that $\lambda^5 + \sum_{i=1}^{5} \kappa_i \lambda^{5-i} = (\lambda+1)^5$ is Hurwitz. First order low-pass filters with a cutoff frequency of 3.14 Hz have been used to filter I_b and V_b, while the output of the function Φ has been filtered with a first order low-pass filter with a cutoff frequency of 1 Hz.

In order to verify that the proposed observer is capable of estimating different values of V_{oc}, such a voltage has been manually changed (by modifying the setting of the voltage generator) at the beginning of each experiment. Fig. 4 depicts the results obtained in three different

[1] The Arduino and Matlab codes that have been used to run the experiments reported in this paper are made available at the following link: https://github.com/Corrado-possieri/StateOfCharge. In fact, the objective of this paper is to develop a robust SOC estimator that can be implemented with low-cost hardware, thus allowing complete reproducibility of the reported results.

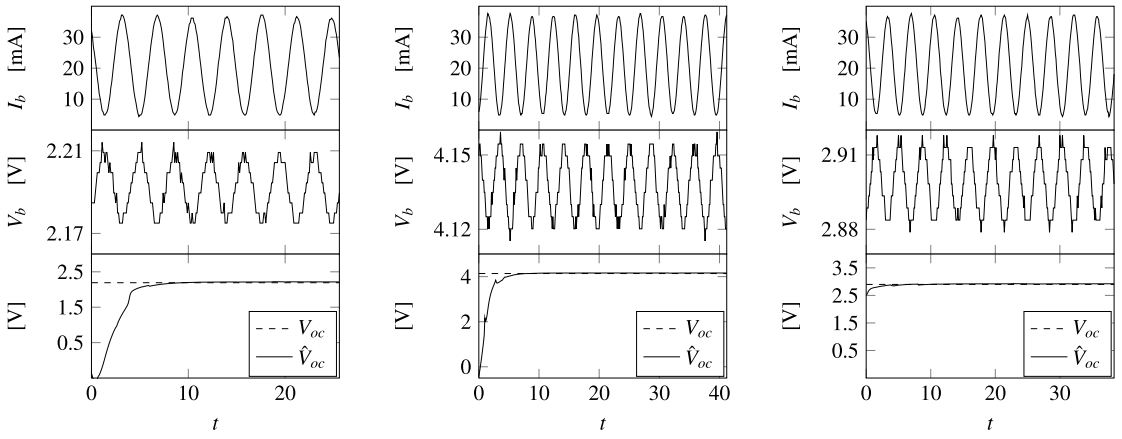

Fig. 4. Results of the first experiment.

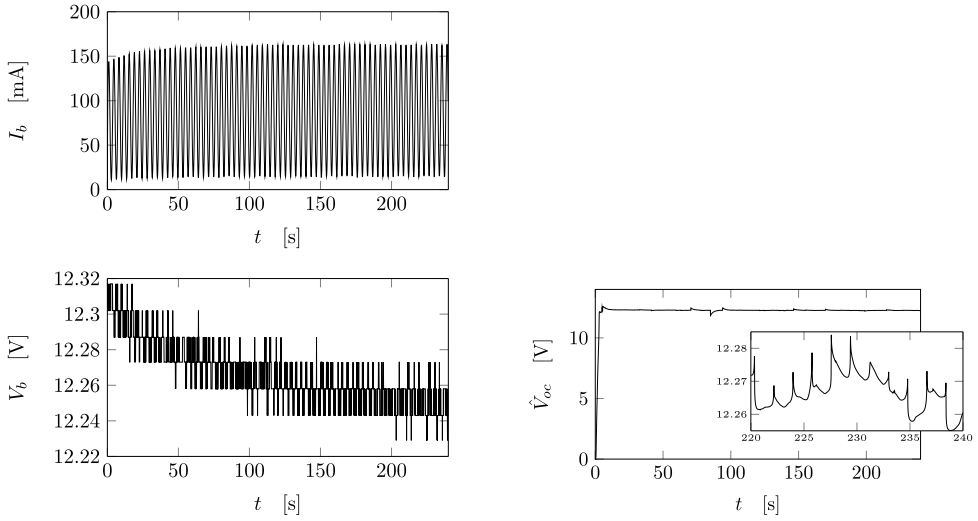

(a) Measured I_b and V_b.

(b) Measured I_b and V_b.

Fig. 5. Results of the first experiments on the real battery.

experiments. In particular, the first and second row of the array of plots reported in Fig. 4 depict the measured I_b and V_b in each experiment, whereas the third row depicts both the actual open-circuit voltage V_{oc} and its estimate $\hat{V}_{oc}$.

As shown by the experimental evidences reported in Fig. 4, the technique illustrated in Section 3 is able to estimate the open circuit voltage V_{oc} based only on measurements of I_b and V_b without requiring any knowledge on the parameters R_c, R_d, R_b and C.

In the following section, the technique given in Section 3 and verified through the experiments reported in this section is used to estimate the open circuit voltage of an actual battery.

5.2. Actual battery

The procedure outlined in Section 5.1 has been used to estimate V_{oc} for an actual battery. The battery that has been used to carry out the experiments is a lead–acid battery with a nominal voltage of 12 V and a capacity of 7 Ah. Such a battery has been plugged to the circuit depicted in Fig. 3 and the same parameters reported for the experiments described in Section 5.1 have been used to estimate the open circuit voltage V_{oc} of the battery in several experiments. Fig. 5(a) depicts the measured I_b and V_b, while Fig. 5(b) depicts the output of the proposed procedure (note that in this experiment the parameter V_{oc} is not measurable and hence the given estimate cannot be compared with the real value of the open circuit voltage).

As shown by such an experiment, the proposed technique gives a consistent estimate of the current value of the open circuit voltage and hence it can be used, together with (2) to determine the current state of charge of a lead–acid battery. Namely, letting $\hat{V}_{oc}$ be the estimated open circuit voltage, $\hat{a}_0$ be the terminal voltage, and $\hat{a}_1$ be $\hat{V}_{oc}$ when $\hat{S} = 1$, an estimate of the current SOC of the lead–acid battery is

$$\widehat{\mathrm{SOC}}(t) = a_1^{-1}(\hat{V}_{oc}(t) - \hat{a}_0).$$

6. Conclusions

In this paper, an approach has been proposed to estimate the state of charge of a battery by measures of the charge/discharge voltage and current on the load, without assuming any knowledge of the battery nominal parameters. The proposed technique has been obtained by combining high gain observers (that have been used to estimate the time derivatives of a given signal) with system embeddings (that have been used to determine explicit formulas relating the time derivatives of the load current and voltage with the open circuit voltage). If the measured signals are affected by significant disturbances, other methods can be used to estimate the time derivatives of the input signals (*e.g.*, the robust differentiator given in Shtessel, Edwards, Fridman, and Levant (2014) without affecting the effectiveness of the method. Interestingly, the proposed technique is genuinely nonlinear and hence it does not require the typical drawbacks of linear, or linearized, approaches, including,

e.g., the requirement for *persistence of excitation* of the load voltage and current. Several experiments have been carried out to validate the theoretical results.

Conflict of interest

None declared.

References

Barbarisi, O., Vasca, F., & Glielmo, L. (2006). State of charge Kalman filter estimator for automotive batteries. *Control Engineering Practice*, *14*(3), 267–275.

Bartlett, A., Marcicki, J., Onori, S., Rizzoni, G., Yang, X. G., & Miller, T. (2016). Electrochemical model-based state of charge and capacity estimation for a composite electrode lithium-ion battery. *IEEE Transactions on Control Systems Technology*, *24*(2), 384–399.

Bhangu, B. S., Bentley, P., Stone, D. A., & Bingham, C. M. (2005). Nonlinear observers for predicting state-of-charge and state-of-health of lead-acid batteries for hybrid-electric vehicles. *IEEE Transactions on Vehicular Technology*, *54*(3), 783–794.

Chang, W. -. Y. (2013). The state of charge estimating methods for battery: A review. *ISRN Applied Mathematics*.

Chiasson, J., & Vairamohan, B. (2003). Estimating the state of charge of a battery. In *Am. Control Conf. (Vol. 4)* (pp. 2863–2868). IEEE.

Chiasson, J., & Vairamohan, B. (2005). Estimating the state of charge of a battery. *IEEE Transactions on Control Systems Technology*, *13*(3), 465–470.

Coleman, M., Lee, C. K., Zhu, C., & Hurley, W. G. (2007). State-of-charge determination from EMF voltage estimation: Using impedance, terminal voltage, and current for lead-acid and lithium-ion batteries. *IEEE Transactions on Industrial Electronics*, *54*(5), 2550–2557.

Corno, M., Bhatt, N., Savaresi, S. M., & Verhaegen, M. (2015). Electrochemical model-based state of charge estimation for li-ion cells. *IEEE Transactions on Control Systems Technology*, *23*(1), 117–127.

Cox, D. A., Little, J., & O'Shea, D. (2015). *Ideals, varieties, and algorithms*. Springer Science & Business Media.

Fuller, T. F., Doyle, M., & Newman, J. (1994). Simulation and optimization of the dual lithium ion insertion cell. *Journal of the Electrochemical Society*, *141*(1), 1–10.

Isidori, A. (1995). *Nonlinear control systems*. Springer-Verlag, Berlin.

Menini, L., Possieri, C., & Tornambe, A. (2015a). Application of algebraic geometry techniques in permanent-magnet DC motor fault detection and identification. *European Journal of Control*, *25*, 39–50.

Menini, L., Possieri, C., & Tornambe, A. (2015b). Sinusoidal disturbance rejection in chaotic planar oscillators. *International Journal of Adaptive Control Signal Processing*, *29*(12), 1578–1590.

Menini, L., Possieri, C., & Tornambe, A. (2016). Switching signal estimator design for a class of elementary systems. *IEEE Transactions on Automatic Control*, *61*(5), 1362–1367.

Pang, S., Farrell, J., Du, J., & Barth, M. (2001). Battery state-of-charge estimation. In *Am. Control Conf. (Vol. 2)* (pp. 1644–1649). IEEE.

Partovibakhsh, M., & Liu, G. (2015). An adaptive unscented Kalman filtering approach for online estimation of model parameters and state-of-charge of lithium-ion batteries for autonomous mobile robots. *IEEE Transactions on Control Systems Technology*, *23*(1), 357–363.

Paschero, M., Storti, G. L., Rizzi, A., Mascioli, F. M. F., & Rizzoni, G. (2016). A novel mechanical analogy-based battery model for SoC estimation using a multicell EKF. *IEEE Transactions on Sustainable Energy*, *7*(4), 1695–1702.

Piller, S., Perrin, M., & Jossen, A. (2001). Methods for state-of-charge determination and their applications. *Journal of Power Sources*, *96*(1), 113–120.

Plett, G. L. (2004). Extended Kalman filtering for battery management systems of LiPB-based HEV battery packs. *Journal of Power Sources*, *134*(2), 252–292.

Possieri, C., & Busetto, A. G. (2017). Observer design for boolean control networks with unknown inputs. *IET Control Theory Applications*, *11*(13), 2116–2121.

Santhanagopalan, S., & White, R. E. (2006). Online estimation of the state of charge of a lithium ion cell. *Journal of Power Sources*, *161*(2), 1346–1355.

Shtessel, Y., Edwards, C., Fridman, L., & Levant, A. (2014). *Sliding mode control and observation (Vol. 10)*. Springer NY.

Smith, K., & Wang, C. -Y. (2006). Solid-state diffusion limitations on pulse operation of a lithium ion cell for hybrid electric vehicles. *Journal of Power Sources*, *161*(1), 628–639.

Sussmann, H. J. (1978). Single-input observability of continuous-time systems. *Theory of Computing Systems*, *12*(1), 371–393.

Tornambe, A. (1992). High-gain observers for non-linear systems. *International Journal of Systems Science*, *23*(9), 1475–1489.